

1 **SUPPLEMENTARY INFORMATION**

2
3 **Flory-Huggins Photonic Sensors**

4
5 Paola Lova,^{1*} Giovanni Manfredi,^{1°} Chiara Bastianini,¹ Carlo Mennucci,² Francesco Buatier de
6 Mongeot,² Alberto Servida¹ and Davide Comoretto^{1#}

7 ¹ Dipartimento di Chimica e Chimica Industriale and ² Dipartimento di Fisica, Università degli
8 Studi di Genova, Via Dodecaneso 31, 16146, Genova, Italy.

9
10 °Present Address: Center for Nano Science and Technology, Istituto Italiano di Tecnologia, Via
11 Giovanni Pascoli 70, 20133 Milano, Italy

12 #E-mail: davide.comoretto@unige.it

13 *E-mail paola.lova@edu.unige.it

14
15
16
17
18 **Table of Contents**

19 1. Full FHPS response to vapor exposure 2
20 2. Assessment of interacting and barrier media 5
21 3. Evaluation of FHPS layer thicknesses 6
22 4. Operative sensing conditions 7
23 Supplementary Reference 8

1 1. Full FHPS response to vapor exposure

2 Supplementary Figure 1 displays the full Flory-Huggins Photonic Sensor (FHPS) optical response
3 to ethanol (EtOH, a-a’), 1-propanol (1POH, b-b’), 2-propanol (2POH, c-c’), and to 1-butanol
4 (1BuOH, d-d’) vapors. At a first look, it is clear that for each alcohol the responses are rather
5 complex and characterized by very different kinetics and spectral behaviors. However, these data
6 allow to easily recognize one analyte from the others, also on the short timescale by themselves.
7 In details, when exposed to EtOH the FHPS shows a response comparable to the one reported in
8 Figure 1 for Methanol (MeOH). The sample photonic band gap (PBG) is initially positioned at
9 ~845 nm, while its second-order replica is at 429 nm (black line in Supplementary Figure 1a and
10 Figure 1). Within 600 min of exposure, the two spectral features red-shift of $\Delta\lambda_{\infty 1 EtOH} = 153 \text{ nm}$,
11 $\Delta\lambda_{\infty 2 EtOH} = 64 \text{ nm}$, in agreement with the data observed for MeOH (Figure 1). The PBGs initially
12 shift with higher velocity than at longer times, as observed in the optical sorption curve reported
13 in Supplementary Figure 2a’’. The analyte uptake increases until $t = 325 \text{ min}$ ($18 \text{ min}^{1/2}$). Then,
14 the position of the PBG oscillates within less than one twentieth of $\frac{\Delta\lambda_t}{\Delta\lambda_\infty}$. This behavior can be
15 assigned to the relaxation and rearrangement of the polymer chains from stresses associated with
16 the swelling induced by the molecule intercalation, and has been described in literature.¹ This
17 phenomenon, has already been demonstrated for CA², and it is known to slow down the permeation
18 process. Indeed, the relaxation corresponds to a chain rearrangement, which results in a slower
19 uptake rate owing to cooperative movements of polymer segments necessary to make larger
20 volume changes. Under this condition the permeation mechanism leads to additional uptake of
21 molecules with a first order kinetic and induces a non-fickian deviation of the sorption curve at the
22 long time scale.³ A similar behavior is visible for all the other molecular species but for MeOH,
23 which shows a continuous increase of analyte uptake until $\frac{\Delta\lambda_t}{\Delta\lambda_\infty} \sim 0.6$, where saturation is reached
24 (Figure 1).

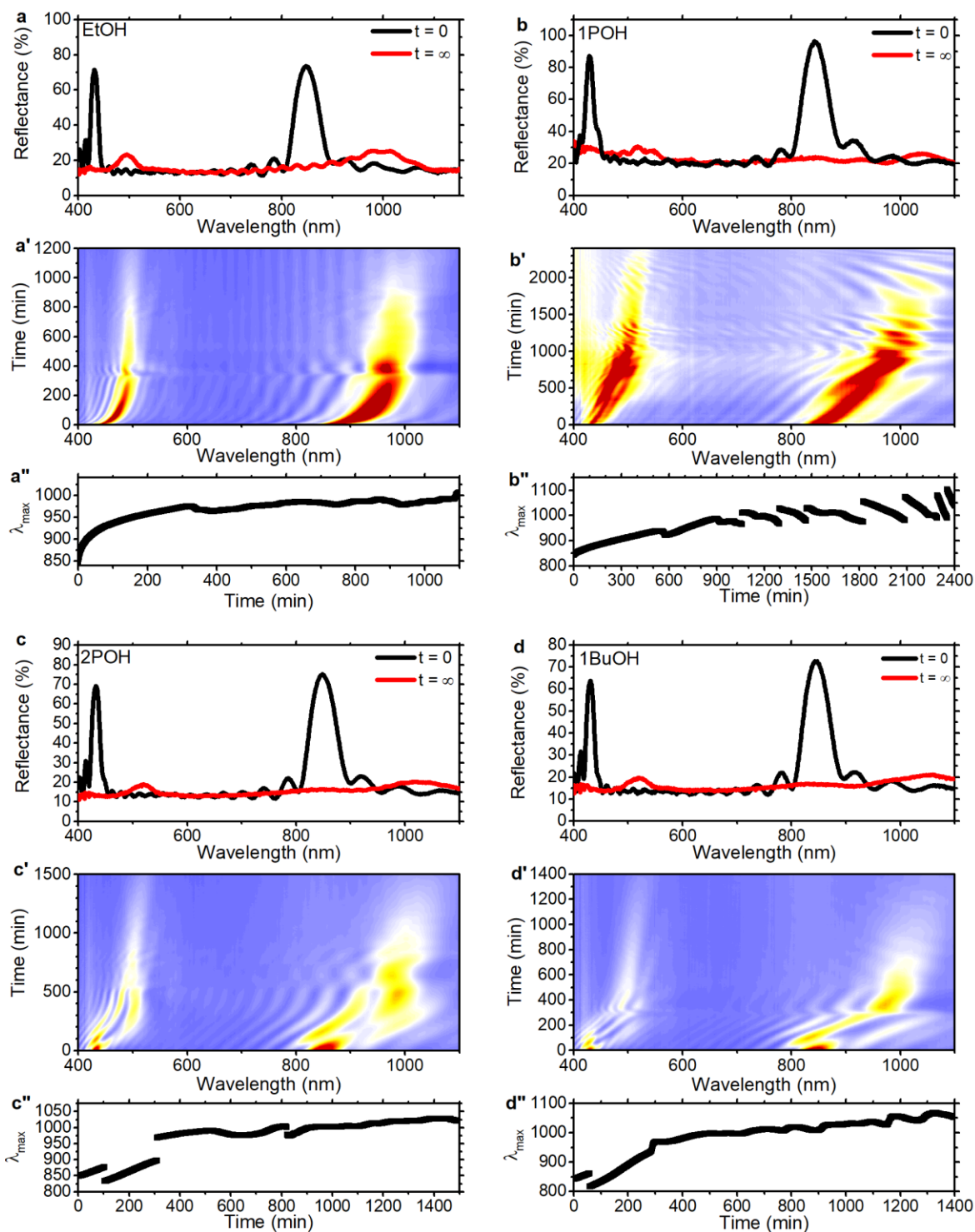
25 Concerning the exposure to 1POH, the kinetics is slower than that for MeOH and EtOH, and a
26 PBG shift of $\Delta\lambda_{\infty 1 1POH} = 180 \text{ nm}$ $\Delta\lambda_{\infty 2 1POH} = 85 \text{ nm}$ is reached within ~ 1500 min (Figure 1 b-
27 b’). In this case, the red-shift of the PBG appears almost monotone till $t=600 \text{ min}$ ($\sqrt{t} > 25 \text{ min}^{1/2}$).
28 Then, the curve starts being discontinuous. Indeed, the PBG shifts to the blue (decrease of $\frac{\Delta\lambda_t}{\Delta\lambda_\infty}$)

1 and then suddenly shifts again to the red part of the spectrum (increase of $\frac{\Delta\lambda_t}{\Delta\lambda_\infty}$, Supplementary
2 Figure 1b' and 1b''). This behavior has been assigned to slow intercalation kinetics, which swells
3 the FHPS layers one by one from the top to the bottom of the sample.^{4,5}

4 In the case of exposure to 2POH, the PBGs reaches a red-shift of $\Delta\lambda_{\infty1\ 2POH} = 182$ nm and
5 $\Delta\lambda_{\infty2\ 2POH} = 90$ nm respectively within 600 min. The entire shift is characterized by a
6 discontinuous behavior. Indeed, the stop-bands initially moves of ~50 nm on the long wavelength
7 side of the spectrum, then suddenly shifts back to the blue in ~100 min (Supplementary Figure 1c'
8 and c'') and then move again to the red monotonically for 200 mins. At this time, the peak suddenly
9 shifts of ~ 70 nm from 900 nm to 970 nm. Here the stationary condition is almost reached. Indeed,
10 the sorption curve of Supplementary Figure 1c'' approaches the plateau. At longer time, we notice
11 other discontinuities in the PBG position assigned to self-stress relaxation.

12 The exposure to 1BuOH displays a similar optical behavior with respect to 2POH. The PBGs
13 undergoes the largest shift at the equilibrium conditions, which corresponds to $\Delta\lambda_{\infty1\ 1BuOH} = 220$
14 nm and $\Delta\lambda_{\infty2\ 1BuOH} = 100$ nm. In Supplementary Figure 3c and c', the position of the PBG moves
15 to the red part of the spectrum discontinuously. After an initial shift from 845 nm to 861 nm, at 50
16 min of exposure the peak suddenly shifts to 820 nm. Then, it linearly moves to 940 nm at ~300
17 mins. At this time, the PBG starts oscillating within a 60 nm interval, corresponding to a $\frac{\Delta\lambda}{\Delta\lambda_\infty} \sim$
18 0.25 in Supporting Figure 1c''. Last, for what concerns 1BuOH we notice again a discontinuity of
19 $\frac{\Delta\lambda_t}{\Delta\lambda_\infty}$ at 50 min ($\sqrt{t} = 7$ min^{1/2}) and relaxation of the polymer chains after 890 min ($\sqrt{t} = 17$ min^{1/2},
20 Supporting Figure 1d-d'').

21 As reported in a previous work⁴ the optical response of the sensors is by itself sufficient to
22 disentangle pure analytes without any further data elaboration. These systems are indeed promising
23 for new generation colorimetric sensors with broad selectivity and tunable sensitivity and lower
24 detection limit⁵ that does not require complex instrumentation and show responses that could be
25 even detected by the naked eye.^{4,5}

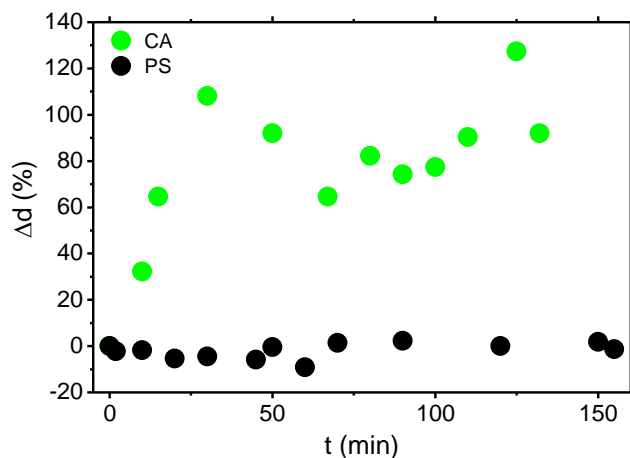


1
 2 **Supplementary Figure 1:** Optical response of the FHPS during the exposure to (a-a'') EtOH, (b-
 3 b'') 1POH, (c-c'') 2POH, and (d-d'') 1BuOH. a-d, Spectra on the FHPS sensor before (black line)
 4 and after (red line) the exposure. a'-d', Contour-plots of the temporal response of the FHPS s. a''-
 5 d'', Sorption curves retrieved from the spectral position of the first order PBG.

2. Assessment of interacting and barrier media

The thicknesses of the PS and the CA single films casted on glass substrates were measured by light interferometry using an interference microscope GBS smart WLI with a 20x interference objective.⁶ The measurements were done placing the sample in a container with a small observation aperture, that does not allow full saturation with the analytes and forbid the measurements with low volatile compounds. On the other hand, it allows to gather qualitative information about the interacting layer of the FHPS with respect to volatile MeOH.

Supplementary Figure 2 reports the polymer swelling as the percent variation with respect to the initial thickness value. The graph shows that when CA is exposed to MeOH (green dots), the layer doubles its thickness within the first 25 minutes of exposure. Conversely, when PS is exposed to MeOH, thickness varies within $\pm 5\%$ with respect to the initial value, that is the instrumental sensitivity. These data suggest that CA is the only polymer interacting with MeOH. Notice that the values obtained for these single layer are not comparable with those of the same polymers within the FHPS, where layer confinement constrains the swelling. Then, these measurements represent the upper limit for the swelling values.

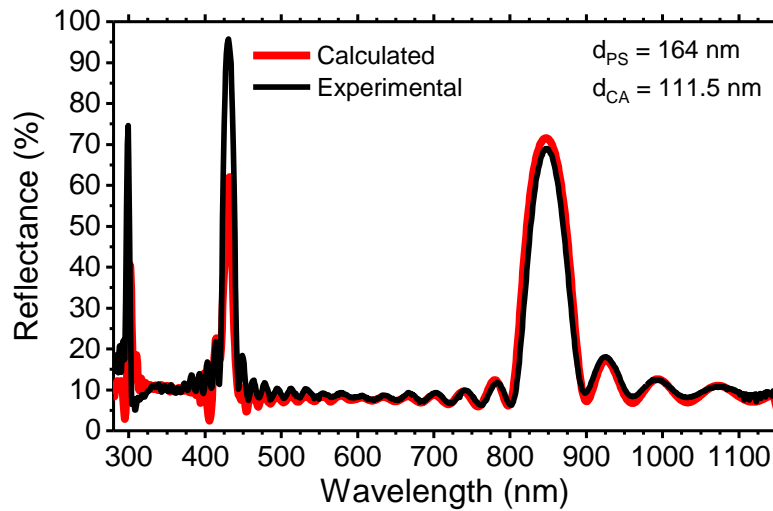


Supplementary Figure 2: Measured PS and CA thicknesses during MEOH exposure by interference microscopy.

3. Evaluation of FHPS layer thicknesses

The reflectance spectrum of the sensors used in this work has already been discussed in Figure 1. Over a more extended range the spectrum shows three maxima of reflection located at 845 nm, 430 nm and 300 nm corresponding to the first order PBG and its two higher order replicas (Supplementary Figure 3). The spectrum background displays a Fabry-Perot pattern typical of DBR structures.

All these spectral features were modelled using a transfer matrix formalism previously reported^{4,5} with the refractive index of PS and CA reported in literature⁷ as inputs and the layer thicknesses as fitting parameters. For this elaboration, the spectrum was analyzed in the range between 290 nm and 1150 nm to fit the largest number of diffraction peaks possible. The red line of Supplementary Figure 3 shows the calculated spectrum, in full agreement with the experimental data. The fitting provides thicknesses of 160 nm for PS and 111.5 nm for CA before the exposures. These data were used to calculate the entire FHPS thickness, necessary for the evaluation of \mathcal{D}_{eff} (Eq. 5), which results 4232 nm.



Supplementary Figure 3: Experimental (black line) and calculated (red line) spectra of the FHPS sensors.

1 **4. Operative sensing conditions**

2 Table 1 reports the operative temperature and analyte concentration.

3

4 **Supplementary Table 1:** Operative condition used during the FHPS exposures

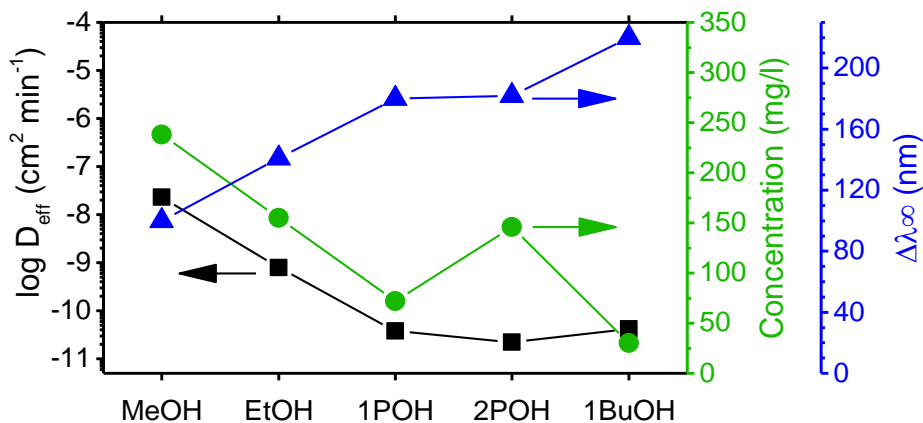
| | T (°C) | C _{vap} (mg/l) |
|--------------|--------|-------------------------|
| MeOH | 26.7 | 238 |
| EtOH | 26.1 | 155 |
| 1POH | 26.0 | 72 |
| 2POH | 25.9 | 146 |
| 1BuOH | 26.8 | 30 |

5

6 $T =$ temperature, $C_{vap} =$ vapor phase concentration.

7

8 Supplementary Figure 4 compares the values of D_{eff} and $\Delta\lambda_{\infty}$ with the analyte concentration.



9

10 **Supplementary Figure 4:** a) Retrieved value of D_{eff} (Eq. 7) for the five alcohols (■), alcohols
11 concentration in the vapor phase (●) and $\Delta\lambda_{\infty}$ (▲).

12

1 **Supplementary Reference**

- 2 1 George, S. C. & Thomas, S. Transport phenomena through polymeric systems. *Prog.*
3 *Polym. Sci.* **26**, 985-1017 (2001).
- 4 2 Perrin, L., Nguyen, Q. T., Sacco, D. & Lochon, P. Experimental studies and modelling of
5 sorption and diffusion of water and alcohols in cellulose acetate. *Polym. Int.* **42**, 9-16
6 (1997).
- 7 3 Berens, A. R. & Hopfenberg, H. B. Diffusion and relaxation in glassy polymer powders:
8 2. Separation of diffusion and relaxation parameters. *Polymer* **19**, 489-496 (1978).
- 9 4 Lova, P. *et al.* Label-free vapor selectivity in poly(p-phenylene oxide) photonic crystal
10 sensors. *ACS Appl. Mater. Interfaces* **8**, 31941–31950 (2016).
- 11 5 Lova, P. *et al.* Polymer distributed Bragg reflectors for vapor sensing. *ACS Photonics* **2**,
12 537-543 (2015).
- 13 6 Kim, S.-W. & Kim, G.-H. Thickness-profile measurement of transparent thin-film layers
14 by white-light scanning interferometry. *Appl. Opt.* **38**, 5968-5973 (1999).
- 15 7 Frezza, L., Patrini, M., Liscidini, M. & Comoretto, D. Directional enhancement of
16 spontaneous emission in polymer flexible microcavities. *J. Phys. Chem. C* **115**, 19939 -
17 19946 (2011).
- 18